Biomaterials 35 (2014) 8487–8495

Contents lists available at ScienceDirect

Biomaterials

journal homepage: www.elsevier.com/locate/biomaterials

Polymeric photosensitizer-embedded self-expanding metal stent for repeatable endoscopic photodynamic therapy of cholangiocarcinoma

Byoung-chan Bae [a, 1], Su-Geun Yang [d, 1], Seok Jeong [c, 1], Don Haeng Lee [b, c, d], Kun Na [a, *], Joon Mee Kim [e], Guido Costamagna [f, g], Richard A. Kozarek [h], Hiroyuki Isayama [i], Jacques Deviere [j], Dong Wan Seo [k], D. Nageshwar Reddy [l]

[a] Department of Biotechnology, The Catholic University of Korea, 43 Jibong-ro, Wonmi-gu, Bucheon-si, Gyeonggi-do 420-743, Republic of Korea
[b] Utah-Inha DDS and Advanced Therapeutics, B-404, Meet-You-All Tower, Songdo-dong, Yeonsu-gu, Incheon, Republic of Korea
[c] Division of Gastroenterology, Department of Internal Medicine, Inha University Hospital, Incheon, Republic of Korea
[d] Department of New Drug Development and NCEED, School of Medicine, Inha University, Incheon, Republic of Korea
[e] Department of Pathology, Inha University Hospital, Incheon, Republic of Korea
[f] Digestive Endoscopy Unit, Department of Surgery, Catholic University, Rome, Italy
[g] Department of Radiology, Catholic University, Rome, Italy
[h] Digestive Disease Institute, Virginia Mason Medical Center, Seattle, USA
[i] Department of Gastroenterology, Graduate School of Medicine, The University of Tokyo, Tokyo, Japan
[j] Department of Gastroenterology, Erasme University Hospital, Brussels, Belgium
[k] Division of Gastroenterology, Asan Medical Center, Seoul, Republic of Korea
[l] Department of Gastroenterology, Asian Institute of Gastroenterology, Hyderabad, India

ARTICLE INFO

Article history:
Received 13 May 2014
Accepted 1 July 2014
Available online 17 July 2014

Keywords:
Cholangiocarcinoma
Photodynamic therapy
Membrane-covered self-expanding metal stent (SEMS)
Bile duct stent
Pheophorbide A

ABSTRACT

Photodynamic therapy (PDT) is a new therapeutic approach for the palliative treatment of malignant bile duct obstruction. In this study, we designed photosensitizer-embedded self-expanding nonvascular metal stent (PDT-stent) which allows repeatable photodynamic treatment of cholangiocarcinoma without systemic injection of photosensitizer. Polymeric photosensitizer (pullulan acetate-conjugated pheophorbide A; PPA) was incorporated in self-expanding nonvascular metal stent. Residence of PPA in the stent was estimated in buffer solution and subcutaneous implantation on mouse. Photodynamic activity of PDT-stent was evaluated through laserexposure on stent-layered tumor cell lines, HCT-116 tumor-xenograft mouse models and endoscopic intervention of PDT-stent on bile duct of mini pigs. Photo-fluorescence imaging of the PDT-stent demonstrated homogeneous embedding of polymeric Pheo-A (PPA) on stent membrane. PDT-stent sustained its photodynamic activities at least for 2 month. And which implies repeatable endoscopic PDT is possible after stent emplacement. The PDT-stent after light exposure successfully generated cytotoxic singlet oxygen in the surrounding tissues, inducing apoptotic degradation of tumor cells and regression of xenograft tumors on mouse models. Endoscopic biliary in-stent photodynamic treatments on minipigs also suggested the potential efficacy of PDT-stent on cholangiocarcinoma. *In vivo* and *in vitro* studies revealed our PDT-stent, allows repeatable endoscopic biliary PDT, has the potential for the combination therapy (stent plus PDT) of cholangiocarcinoma.

1. Introduction

Cholangiocarcinoma is a rare but fatal malignant neoplasm, which arises from the epithelium of intra- or extra-hepatic bile ducts [1,2]. Globally, cholangiocarcinoma accounts for 3% of gastrointestinal tumors and approximately 10–15% of all primary liver tumors [3,4]. The annual incidence of cholangiocarcinoma in western countries is approximately 1–2 cases per 100,000 individuals, and this incidence is steadily increasing [5,6]. East Asia has a much higher incidence (6–8 cases per 1000 individuals), and Northeast Thailand has the highest incidence at 94.8–97.4 cases per 1000 men [7]. In this area, cholangiocarcinoma is largely associated with hepatocellular carcinoma.

Cholangiocarcinoma is a latent tumor; routine diagnosis by blood test, MRI, CT and endoscopy may not detect early neoplastic

* Corresponding author. Tel.: +82 2 2164 4832; fax: +82 2 2164 4865.
E-mail address: kna6997@catholic.ac.kr (K. Na).
[1] Authors are equally contributed on this works.

http://dx.doi.org/10.1016/j.biomaterials.2014.07.001
0142-9612/

bile duct changes [2,8]. Thus, the diagnosis of cholangiocarcinoma so highly counts on symptoms than more than 70% of cases are on inoperable stage. Optional therapies for the unresectable cholangiocarcinoma are very confined [9–11]. The 5-year survival rate of the resectable cholangiocarcinoma is approximately 20–40%, but the median survival of unresectable cholangiocarcinoma is only around 3 months [12,13]. In any cases, one of the major concerns for cholangiocarcinoma is bile duct occlusion, where the growing cholangiocarcinoma blocks the bile duct, leading to jaundice, cholangitis, and hepatic failure. Surgical biliary bypass, an optional treatment for biliary obstruction, can cause serious postoperative complications and increase perioperative morbidity and mortality. In contrast, biliary stent allows rapid and efficient relief of symptoms without any life-threatening complications. Palliative biliary drainage using a biliary stent extends the median survival up to 6 months [14,15]. A self-expanding metal stent (SEMS) is the most technically advanced biliary stent, and has been shown to be clinically effective for over a number of years [16,17]. The knitted metallic mesh of SEMS generates axial and radial forces, which exert resistant strength against tumor infiltration. However, tumor in-growth through the stent cells eventually leads to re-occlusion of the bile duct. Re-occlusion occurs in 5–38% of patients, and the median time of patency ranges from 2.5 to 6.5 months [18,19]. Thirty-one percent of patients underwent more than one re-intervention, which increases the risk of cholangitis, discourages patient compliance, and increases hospitalization expenses. Designing more functional stents, which can prevent tumor infiltration and eventually challenge therapy, is compelling, and a number of researchers have designed more advanced types of stents. Among them, designing drug-eluting stents (DES), a promising breakthrough for re-stenosis, has been attempted several times [20]. Almost a decade ago, cardiovascular stents with low-dose paclitaxel, sirolimus, and everolimus were developed to prevent infiltration of smooth muscle cells. The clinical success of vascular DES encouraged the expansion of drug-eluting technology and the invention of other medical devices [21,22].

Recently, drug-eluting technology using high-dose paclitaxel, 5-FU, and other drugs, was applied to gastrointestinal stents for the treatment of malignant hyperplasia [23,24]. The first clinical trial was performed at Guy's Hospital in London. Paclitaxel-eluting nonvascular DES was used in 21 patients with unresectable adenomatous esophageal cancer [25,26]. However, no clinical effectiveness was observed. More recently, the efficacy of gemcitabine-eluting membrane-covered SEMS was evaluated in a canine model of unresectable adenomatous esophageal cancer [27].

Intra-luminal photodynamic therapy (PDT) is another possible treatment for cholangiocarcinoma. Endoscopic laser probe enables direct photodynamic treatment of cholangiocarcinoma after intravenous photosensitizer injection. Recent clinical data showed that PDT increased survival rates in cholangiocarcinoma patients. Furthermore, combination therapy of PDT and SEMS synergistically improved survival rates [28–31]. Witzigmann et al. evaluated combination PDT and stent therapy in 184 patients with hilar cholangiocarcinoma. They reported that the survival time of the PDT plus stent group was twice that of the stent alone group [28]. Another clinical trial comparing biliary stent alone and stent plus PDT for perihilar cholangiocarcinoma was terminated early because the survival benefit of combination therapy was significantly higher when compared to the stent alone group [31].

In this study, we designed a photosensitizer-embedded membrane-covered SEMS (PDT-stent). Based on our design, PDT-stent may generate cytotoxic singlet oxygen under endoscopic light activation, precipitate the regression of surrounding malignant tissue, extend stent patency, and eventually increase survival rate. Pheophorbide A (Pheo-A), a plant-derived photosensitizer, was selected, chemically conjugated with pullulan acetate (polymerized pheophorbide A; PPA), and embedded in stent-covering polyurethane membranes (PPA-stent). Free Pheo-A (FPA) was also embedded in a similar manner and was used as the control stent (FPA-stent).

In vitro photodynamic activities (i.e., singlet oxygen generation, cytotoxic activity, and sustained retention of PPA in the covering membrane) of PDT-stents were evaluated. *In vivo* tumor regression after PDT-stent therapy was tested on tumor-xenograft mouse models. Furthermore, endoscopic PDT was performed on the normal bile duct of mini pigs after the emplacement of PPA-stent.

2. Materials and methods

2.1. Synthesis of polymeric photosensitizer

In this study, pullulan, polymeric carrier of photosensitizer, was acetylated and then conjugated with photosensitizer using a method previously reported by our group (see online Supplementary method and Scheme 1) [32,33].

2.2. PDT-stent fabrication

Polymeric or free form of photosensitizer was respectively embedded into the stent membrane using a dip coating method (see online Supplementary Fig. S5) [24,27]. PPA or FPA was dissolved in THF solution and mixed again with a polyurethane solution. Pheo-A (4 mg) and polyurethane (5 g) were dissolved in 100 mL of THF dipping solution. SEMS was dipped in the dipping solution for 1 min, slowly drawn out, and air-dried for 1 day at room temperature. Both PPA membrane layered stents (PPA-stent) and FPA membrane layered stents (FPA-stent) were fabricated in the above manner. The Pheo-A concentration in each stent was 40 $\mu g/cm^2$ of the membrane.

After stent fabrication, stent membranes were observed and analyzed by performing field emission scanning electron microscopy (FE-SEM) (Hitachi S-4800, Tokyo, Japan). Stent membranes were sliced into small pieces, mounted, sputter-coated with gold using an ion coater, and then observed at an accelerating voltage of 20 kV.

2.3. Estimation of effective time duration for repeatable PDT after stenting

Based on our design, endoscopic PDT is repeatable as long as the photosensitizer perseveres in the stent. In this study, we estimated *in vivo* and *in vitro* retention of photosensitizer (free Phoe-A and polymerized Phoe-A) in stent. For the *in vitro* assay, metal stents were fragmented into 4 square meshes, dip-coated with photosensitizer, and air-dried. PPA- and FPA-stents were then immersed into PBS buffer under shaking conditions at 37 °C. The release and residual amount of Pheo-A was estimated using a fluorescence spectrophotometer (RF-5301PC; Shimadzu, Japan). Stent fragments, immersed in buffer, were periodically taken out, and photo-fluorescence intensity was observed on an fluorescence image Station 4000 MM (Kodak, New Haven, CT) with a special C mount lens and a long wave emission filter (600–700 nm; Omega Optical, USA) [34].

In vivo estimation was performed after subcutaneous implantation of stent. PPA- and FPA- stent membranes, contained 40 $\mu g/cm^2$ of Pheo-A, were subcutaneously implanted under the skin of BALB/c nude mice. Time-dependent fluorescence intensity were measured for 2 months using an Image Station 4000 MM (Kodak, New Haven, CT). All the animal studies were approved by the Institutional Animal Care and Use Committee.

2.4. Cell lines

HeLa, NIH3T3, and HCT-8 cells were purchased from the Korea Cell Line Bank (Seoul, Korea) and maintained in a humidified 5% CO_2 incubator at 37 °C in RPMI 1640 medium supplemented with 10% heat-activated bovine serum, 100 IU mL^{-1} penicillin and 100 mg mL^{-1} of streptomycin.

2.5. Photodynamic activities of PDT-stents on cancer cell lines

FPA- and PPA-stents under the *in vitro* retention study (see above) were periodically recovered from buffer solution and introduced to cell lines for photodynamic treatment. Briefly, HeLa, NIH3T3, and HCT-116 cells were seeded onto 12-well culture plates at 1×10^5 cells/well. After an overnight incubation, FPA- and PPA-stents were placed on top of cells and activated by an exposure to visible light (670 nm, 1.2 J/cm^2 of energy strength) using a copper vapor laser (Institute of Electronics, Beijing, China). After the light exposure, the cells were stained with 0.4% trypan blue solution for 3 min at room temperature for observation. Live/dead cell staining was performed using a commercial kit (Molecular Probes, Inc., Eugene, OR), and the stained cells were observed under a fluorescence microscope (Carl Zeiss Microscope System, Jena, Germany).

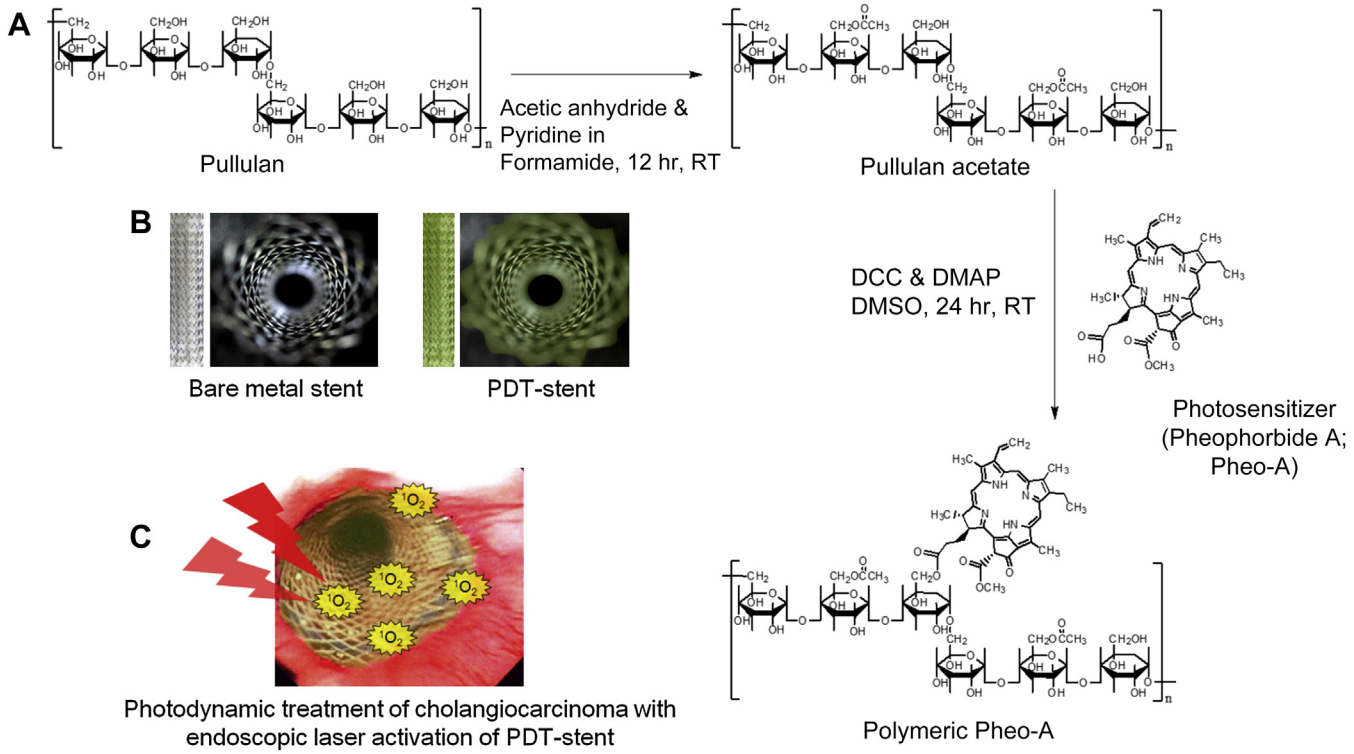

Scheme 1. Overall scheme and conceptual image of PDT-stent. A) Chemical synthesis of polymeric photosensitizer (Pullulan acetate-conjugated Pheophorbide A; PPA). B) Conventional bare metal stent and PPA-coated PDT-stent. C) Generation of cytotoxic singlet oxygen ($^1O_2$) under endoscopic laser activation.

2.6. Photodynamic activities of PDT-stents on HCT-116 tumor xenograft mouse model

HCT-116 tumors (human colorectal carcinoma) were subcutaneously established on the flank of mice. When the tumor reached an average diameter of approximately 6 mm, FPA- or PPA-stent membranes (40 μg/cm^2 Pheo-A) were surgically implanted under the tumor. Twenty mice were divided into 5 groups as follows: 1) PU membrane; 2) FPA-stent membrane with PDT-laser; 3) FPA-stent membrane without PDT-laser; 4) PPA-stent membrane with PDT-laser and 5) PPA-stent membrane without PDT-laser. After implantation, the mice with PDT groups were directly exposed to a copper vapor laser (670 nm, 100 J/cm^2, see online Supplementary Fig. S7). Tumor size was measured every 2 days using Vernier calipers (Mitutoyo Co., Japan). Volume was calculated using the formula $V = [a \times (b \times b)]/2$, with a the largest and b the smallest diameter of tumor [35]. Two weeks after the laser treatment, the tumor tissues were introduced to hematoxylin and eosin (H&E) staining and terminal deoxynucleotidyl transferase (TdT)-mediated dUTP nick end labeling (TUNEL) staining after fixation in 4% paraformaldehyde.

2.7. Endoscopic PDT after emplacement of PDT-stents on mini pigs' bile duct

Conventional stents (Taewoong medical co. Seoul, Korea) or PPA-stents were introduced to the bile duct of mini pigs (*Sus scrofa*, 25–30 kg) under anesthesia (see online Supplementary Figs S8 and S9). Different energy levels of PDT (40, 70, and 150 J/cm^2) were performed using an endoscopic laser. Two days after irradiation, bile ducts were recovered for histology.

3. Results

3.1. Photo-fluorescence images of PDT-stent

In this study, photodynamic activity of stents based on photo-fluorescence imaging using an Image Station 4000 MM (Kodak, New Haven, CT) was analyzed. The excited photosensitizer in triplet

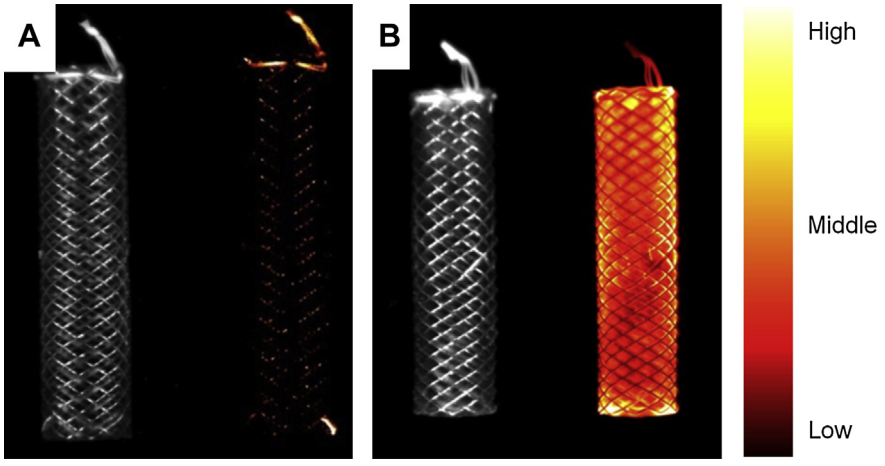

Fig. 1. Photo-fluorescence of PPA-coated self-expandable metal stent: DIC and photo-fluorescence images of bare metal stent (A) and PDT-stent (B) under photo-excitation.

state illuminates photo-fluorescence. Therefore photodynamic activity of Pheo-A can be assumed based on the photo-fluorescence intensity. PPA-stents showed homogenous and strong photo-fluorescence (Fig. 1B and Fig. S6) across the stent. No photo-fluorescence was observed with conventional SEMS (Fig. 1A).

3.2. Effective time duration for repeatable stent-PDT after stenting

Based on our design, PDT-stent is capable of repeatable photodynamic treatments during the patency. We supposed polymeric photosensitizer (PPA), rather than free photosensitizer (FPA), could beneficially retain in the stent longer time after stent emplacement on bile duct. And which eventually allows repeatable endoscopic PDT.

In vitro retention of PPA and FPA in the stent was estimated in shaking buffer at 37 °C (Fig. 2A). Approximately 80% of PPA was retained in the stent and maintained strong photo-fluorescence at the end of the immersion study (Fig. 2C). In contrast, FPA-stents showed a rapid loss of free Pheo-A, and more than 60% of Pheo-A was dissolved out during the 2-months' of immersion. Identical results were observed in photo-fluorescence imaging (Fig. 2B).

Surface morphology of stent membranes during the immersion study was observed by FE-SEM and shown in Fig. 2D and E. SEM analysis verified that stent membranes, containing PPA, had smooth and uniform surfaces and consistently maintained surface smoothness until the end of immersion study. Free Pheo-A initially formed a multi-dented membrane, and surface irregularity increased during the immersion in buffer. Bile duct stents are easily occluded with sludge consisting of proteins, bilirubin, bacteria, and food debris. Plastic biliary stents have relatively short patency due to biliary sludge accumulation. The major cause of biliary sludge accumulation is surface irregularities and hydrophobicity of the stent surface [36,37]. SEMS, relatively has longer patency, is also affected by membrane characteristics. Teflon has been preferentially used for stent membrane because of its excellent mechanical strength against corrosive bile acids. However, biliary sludge easily congregates on the woven structure of Teflon and precipitates restenosis. As shown in Fig. 2E, PPA, formed and maintained smooth stent membrane, possible prevents sludge accumulation and helps elongating the patency.

In vivo retention of FPA and PPA in stent was observed under the skin of Balb/c nude mice and shown in Fig. 3A and B. FPA-stent rapidly lost more than 60% of the initial fluorescence intensity during 4 days of implantation. Polymerized Pheo-A (PPA), however, maintained initial fluorescence for at least 7 days, after which fluorescence was gradually lost. *In vivo* environments precipitated the loss of Pheo-A, especially with FPA-stents. Those *in vitro* and *in vivo* data strongly suggests our PPA-stent, contains polymerized Pheo-A, allows in-stent PDT in repeatable manner at least for 2 months, and which must be a great therapeutic benefit of our stent design as proved in previous clinical studied (stent plus PDT).

3.3. In vitro photodynamic activities of PPA- and FPA-stents

PPA- and FPA-stents during the immersion study were periodically sampled, introduced to cancer cell lines, and activated with a copper vapor laser (670 nm, 1.2 J/cm^2). The laser-exposed cells were stained with 0.4% trypan blue solution and a Live/Dead Viability/Cytotoxicity Assay Kit (Molecular Probes Inc., Eugene, OR). Trypan blue staining showed HeLa, NIH3T3, and HCT-8 cell lines were, especially in contacting region, stained blue, and its' blue intensity was maintained for 28 days when treated with PPA-stent (Fig. 4A). The cellular death rate of HCT-8, NIH3T3, and HeLa cells, treated with FPA-stents after 4 weeks of immersion, decreased to 50% (Fig. 4B). The Live/Dead Viability/Cytotoxicity assay showed results comparable with that of methylene blue staining (Fig. 4C). The above results, together with the *in vitro* immersion study, proved that PPA more stably resided and maintained photodynamic activity in polyurethane membranes.

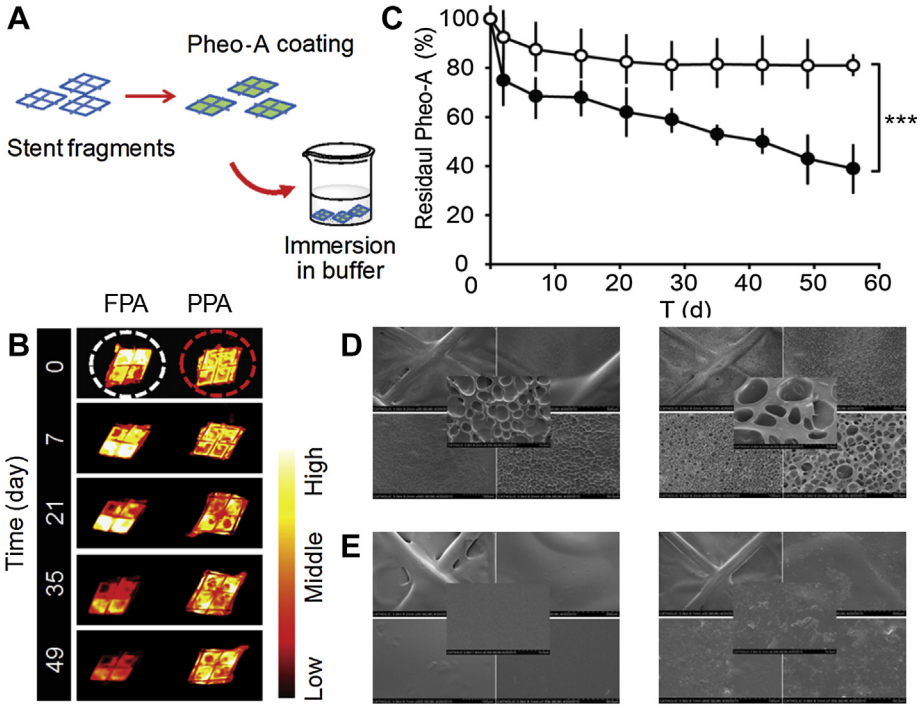

Fig. 2. Time-duration photodynamic activity of PDT-stent under the elution buffer. A) PDT-stent fragments were immersed in buffer and periodically taken for the studies. B) Photo-fluorescence images of FPA-stent and PPA-stent under *in vitro* buffer elution. C) Quantification of fluorescence intensity of PPA- (white circle) and FPA-coated stents (black circle). D) FE-SEM observation of FPA-stent membrane, before (left panel) and after (right panel) the retention study in buffer solution. E) FE-SEM observation of PPA-stent membrane, before (left panel) and after (right panel) the retention study in buffer solution. FE-SEM magnification was 30×, 100×, 300×, 1000×, and 5000×, respectively. ***; $p < 0.001$.

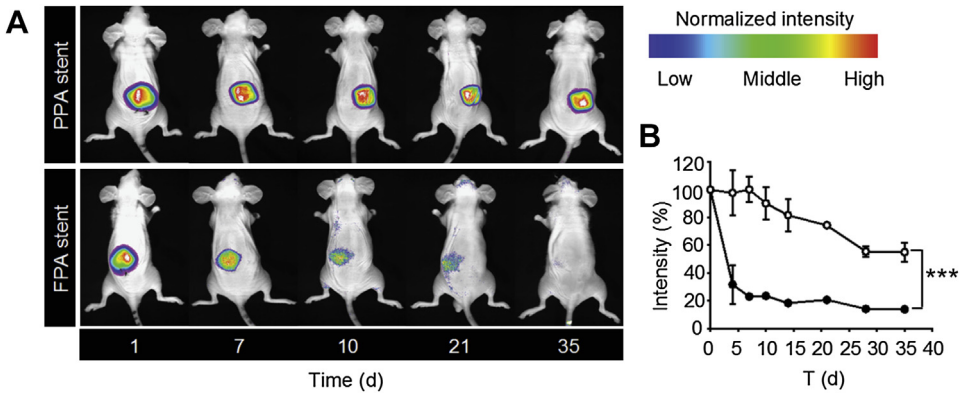

Fig. 3. Time-duration photodynamic activity of PDT-stent after subcutaneous implantation on mouse. A) Photo-fluorescence images of subcutaneously implanted PPA- and FPA-stent membranes. B) Photo-fluorescence intensity of subcutaneously implanted PPA- and FPA-stent membranes. ***; $p < 0.001$.

3.4. In vivo photodynamic activities of PPA- and FPA-stent on subcutaneous tumor

Tumor growth inhibition of PDT-stents was estimated using a subcutaneous tumor-xenograft mouse model bearing HCT-116 cells (human colon cancer cells). Fig. 5A–C show that PPA-stent with laser exposure significantly inhibited tumor growth in comparison with other treatments ($p < 0.001$, compared to PPA w/o light) without weight loss. H&E staining of tumor tissues were correspondent with tumor regression study (Fig. 5D). The control group and laser-untreated groups maintained intact tissue structure, PPA-stent group with laser exposure induced severe deformation of cellular structures. Slight alterations of cellular structure were observed in FPA-stent group with laser exposure. TUNEL and PCNA staining were correspondent with H&E staining. TUNEL staining revealed that tumor cells treated with the PPA-stent plus laser underwent massive apoptosis. PCNA staining also proved that proliferation of tumor cells was inhibited when treated with PPA plus laser.

3.5. Endoscopic photodynamic activities of PPA-stent on normal bile duct of micro pig

PDT-stents was implanted on normal bile duct of mini pigs (*S. scrofa*, 25–30 kg) and irritated with endoscopic light probe. Two days after irradiation, bile duct was recovered for histology (Fig. 6). Bile duct treated with control stents (membrane-covered SEMS) showed denuded mucosa with marked inflammation and hemorrhage (Fig. 6A). This inflammation, which was suggestive of mechanical injury, is commonly observed after placement of a conventional membrane-covered stent [38]. PPA-stent without laser exposure also showed similar mucosal changes as the control group (Fig. 6B).

Tissues after endoscopic PDT are shown in Fig. 6C–F. The degree of mucosal destruction escalated with the increased energy level of laser. Slight injury of the mucosal layer was observed in the 40 J/cm^2 group. The 70 J/cm^2 group showed severe inflammation and loss of the muscle layer, while the 150 J/cm^2 group showed a similar level of injury as observed in the 70 J/cm^2 group. There was no evidence of trans-mural perforation.

4. Discussion

Cholangiocarcinoma prognosis, especially in unresectable cases, is very poor. Mean survival of patients with unresectable cholangiocarcinoma is generally no more than 12 months. Biliary stent is recommended when the expected patient survival is less than 4 months or if the stent cost is 50% less than the procedural cost of endoscopic retrograde cholangiopancreatography (ERCP) [39]. The reported patency of a conventional metal stent is less than 6 months [40].

In this study, we proposed a new therapeutic modality for cholangiocarcinoma, PDT-stent, which allows repeatable and interventional photodynamic therapy directly to the tumoral bile duct without systemic injection of photosensitizer. After emplacement of PDT-stent, laser-emitting endoscopic probe, guided in the luminal side of the stent, emits laser (670 nm). The laser-activated PDT-stent delivers energy to oxygen in tumoral tissue, forms cytotoxic singlet oxygen, and induces apoptosis of malignant cells (Scheme 1C). And which process can be performed in repeatable ways at least the photosensitizer retains in the stent membranes.

The photosensitizer was polymerized in this study to increase retention in the stent membrane. Pullulan was selected as the polymeric carrier of photosensitizer. Pullulan is biodegradable and water-soluble polysaccharide produced by the black yeast *Aureobasidium pullulans* and has been widely selected for a drug carrier by itself or after chemical modification (Scheme 1A) [41,42]. In this study, pullulan acetate, the hydrophobic form of pullulan, was chemically conjugated with Pheo-A (PPA, Scheme 1A) and embedded in stent-covering membrane. PPA contains 1.71 acetyl groups and 2.5 Pheo-A molecules per maltotriose unit (see online Supplementary Fig. S1). *In vitro* and *in vivo* study proved polymerized photosensitizer lengthened the retention stability in the stent-covering membrane in comparison with free Pheo-A (Figs. 2 and 3). Based on the retention study, we inferred that multiple PDT is possible at least for 2 months. In this manner, the PDT-stent described in this study could increase stent patency as well as patient survival.

Pheo-A, the breakdown product of chlorophyll, absorbs energy under violet-blue (350–450 nm) and orange-red (550–700 nm) laser exposure and transfers energy to molecular oxygen (O_2) which in turns transforms to triplet state ($^3O_2$) and then to the highly reactive singlet state ($^1O_2$*; *represents electronically excited state) [43,44]. This cytotoxic singlet oxygen readily reacts with electron-rich cellular molecules such as DNA, amino acids, and unsaturated lipids, and induces apoptosis of malignant cells.

Hackbarth et al. studied the photodynamic properties of Pheo-A dendrimer (Pheo-DAB) [45]. Pheo-DAB is formed by conjugation of Pheo-A with diaminobutane poly-propylene-immine dendrimer (DAB). Approximately 12–13 molecules of Pheo-A were conjugated per single dendrimer. Originally, Pheo-A generates a singlet oxygen quantum yield of approximately 0.52, which is much higher than the 0.2 yield of a commercialized photosensitizer (Photofrin II). However, Pheo-DAB failed to show any improvements in singlet

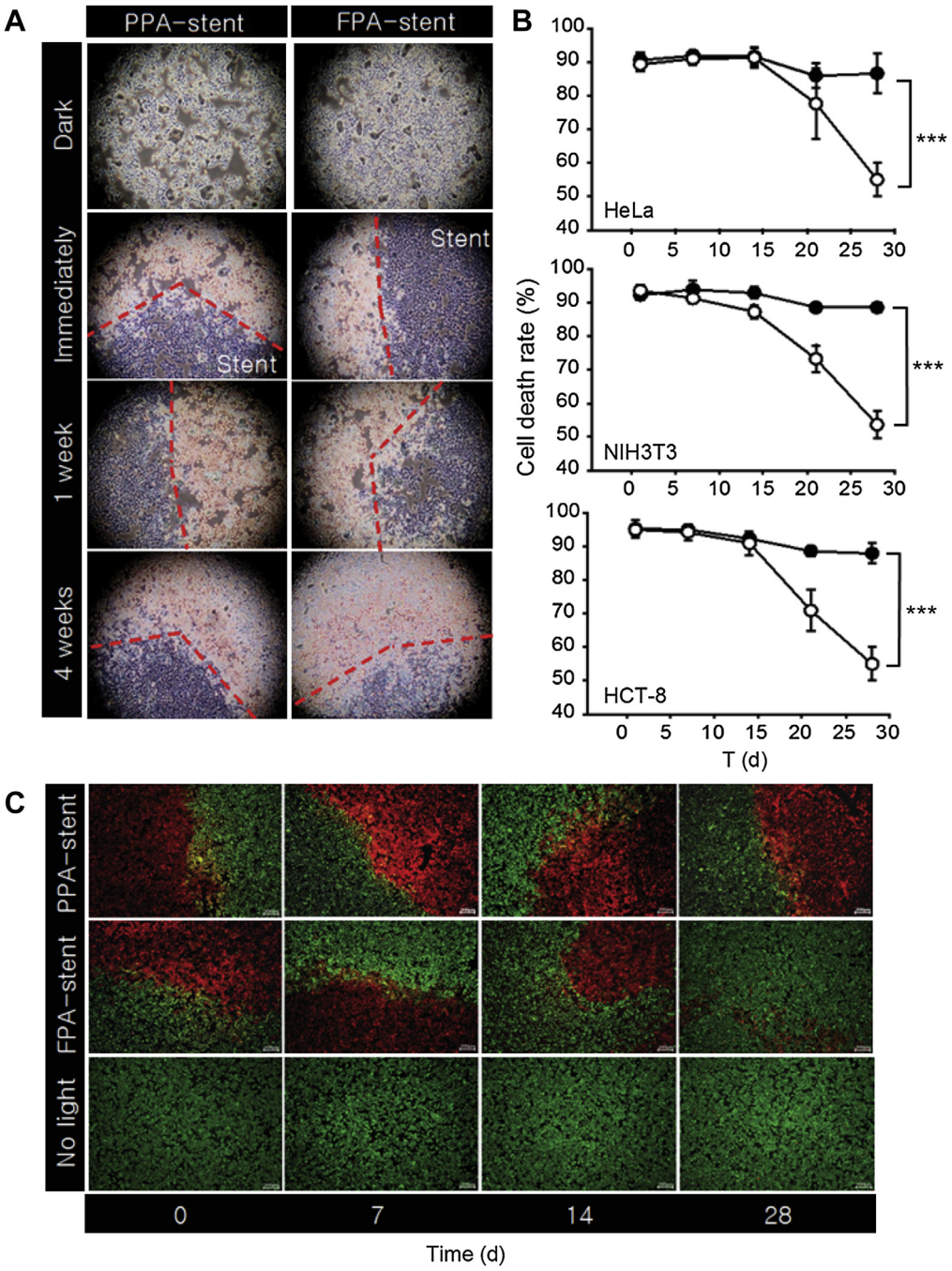

Fig. 4. *In vitro* photodynamic activities of PPA- and FPA-stent against tumor cell lines. FPA- and PPA- stents were periodically recovered during the retention study (0, 7, 14 and 28 days of immersion in buffer, experimental Section 2.5), layered on the cell lines and laser-activated (10 mW/cm^2 laser for 5 min). A) Trypan blue staining of HCT-8 cells covered with PPA-stent (left panel) and FPA-stent (right panel) after light irradiation. B) Photodynamic treatment induced-cell death of HeLa, NIH3T3, and HCT-8 cells. C) Live and dead cell staining of HCT-116 cells after photodynamic treatment. Live cells: green fluorescence (calcein AM); dead cells: red fluorescence (EthD-1). Scale bar = 200 μm ***; $p < 0.001$. (For interpretation of the references to colour in this figure legend, the reader is referred to the web version of this article.)

oxygen quantum yield (0.52 vs. 0.3 for Pheo-A and Pheo-DAB). The fluorescence lifetime was also shorter than expected (5.7 ± 0.2 vs. 4.9 ± 0.3 ns for Pheo-A and Pheo-DAB), but initially-formed singlet oxygen triggered break-out of Pheo-A from dendrimers and full recovery of photodynamic activity [45]. Unlike Pheo-DAB, PPA, formulated from covalent coupling between Pheo-A and PA, showed only slight changes in UV absorption spectra. Absorption band widths were slightly increased, and the Q-band also showed a diminutive bathochromic shift (Supplementary Fig. S3A). λ_{max} at 670 nm was decreased after polymer conjugation by 14% (0.7–0.5) at 0.2 mol of Pheo-A in DMSO. λ_{max} of emission fluorescence (ex; 612 nm, em; 670 nm) of PPA in DMSO was decreased by 25% (Supplementary Fig. S3B). Based on the UV and fluorescence spectroscopy, PPA may not be affected by any quenching mechanism, i.e., förster resonance energy transfer or static quenching. Pullulan is a linear polymer and the degree of substitution with Pheo-A was 0.02%, indicating that PPA possessed enough molecular space to minimize quenching.

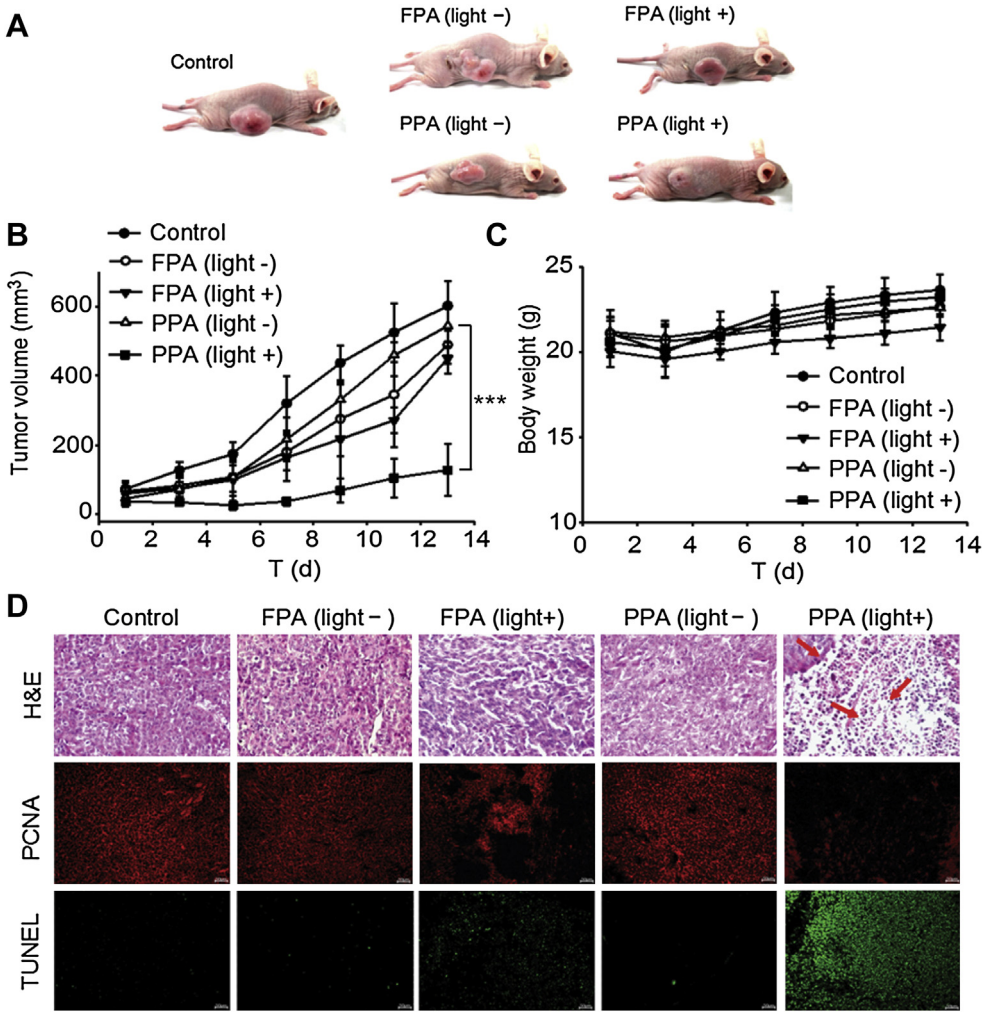

Fig. 5. *In vivo* photodynamic activities of PPA- and FPA- stent membranes. A) Representative whole body images of HCT-116 tumor-bearing mice, 13 days after the photodynamic treatment of PPA- and FPA- stent membranes with or without laser activation. B) Tumor growth of HCT-116 tumor-bearing mice treated with; ●: control, ○: FPA membrane without light, ▼: FPA membrane with light, △: PPA membrane without light, ■: PPA membrane with light. Tumor volumes were measured for 13 days post-treatment. (C) Body weight was measured for 13 days post-treatment. All data ($n = 4$) represent means ± SEM. ***; $p < 0.001$. D) Immunohistochemical analysis of HCT-116 xenografts in tumors treated with PPA- or FPA- stent membranes. Tumors were analyzed by H&E (magnification; 400×, scale bar = 20 μm), PCNA, and TUNEL staining (magnification; 200×, scale bar = 50 μm).

Our data confirmed that PPA-stent is photodynamically active against subcutaneous tumors. In the case of advanced or unresectable gastrointestinal tumors, palliative stent treatment to ameliorate biliary drainage is essential. As suggested in our experiment, stent treatment, combined with the polymeric photodynamic modality, has the potential to facilitate drainage and prevent subsequent stent occlusion. Furthermore, PDT induces tumor regression, not only by generation of cytotoxic singlet oxygen, but also by subsequent induction of NF-κB, pro-inflammatory cytokines (IL-1β, IL-6, IL-8, IL-10, and others) and infiltration of immune cells [46–48]. These serial reactions boost the therapeutic efficacy of PDT [47]. Supplementary Fig. S10 shows the PDT-stent-induced expression of pro-inflammatory cytokines. Immunohistochemical analysis in HCT-116 xenografts of tumors treated with PPA-stent showed increased expression of IL-2, IL-6, IL-10, TNF-α, and G-CSF. Gollnick et al. have demonstrated that a secondary PDT with a split-dose regimen (initial low-dose and secondary high-dose at a 10 day time interval) increased the activity of tumor-specific T cells and antitumor immunity. However split-dose regimen is not always practical because of systemic injection of photosensitizer critically confine patient's outdoor activities at least for one week after the injection. In this regard, repeatable endoscopic PDT, based on our PDT-stent design, has the therapeutic advantages [49].

Endoscopic intervention study in a mini pig strongly proved the feasibility of our PDT-stent for future clinical studies. PPA-stent after laser treatment showed mucosal inflammation and apoptotic cell death of the sub-mucosal layer. Our experiments suggested the maximum photodynamic activity of the PPA-stent was achieved at 70–150 J/cm^2 of photo-activation. Though this experiment was conducted with normal bile duct, the data are relevant in assuring that PDT-stents exerts photodynamic activity and therapeutic effectiveness in cholangiocarcinoma. The optimal laser strength and the time schedule for the multiple PDTs can be more precisely determined in further clinical trials.

5. Conclusions

Our study suggests an additional option for the treatment of cholangiocarcinoma. Covered SEMS with polymeric photosensitizer functions in palliative treatment for biliary drainage and also has potential as a repeatable and efficient PDT therapy. Repeatable endoscopic PDT via the PDT-stent provides a potentially clinically

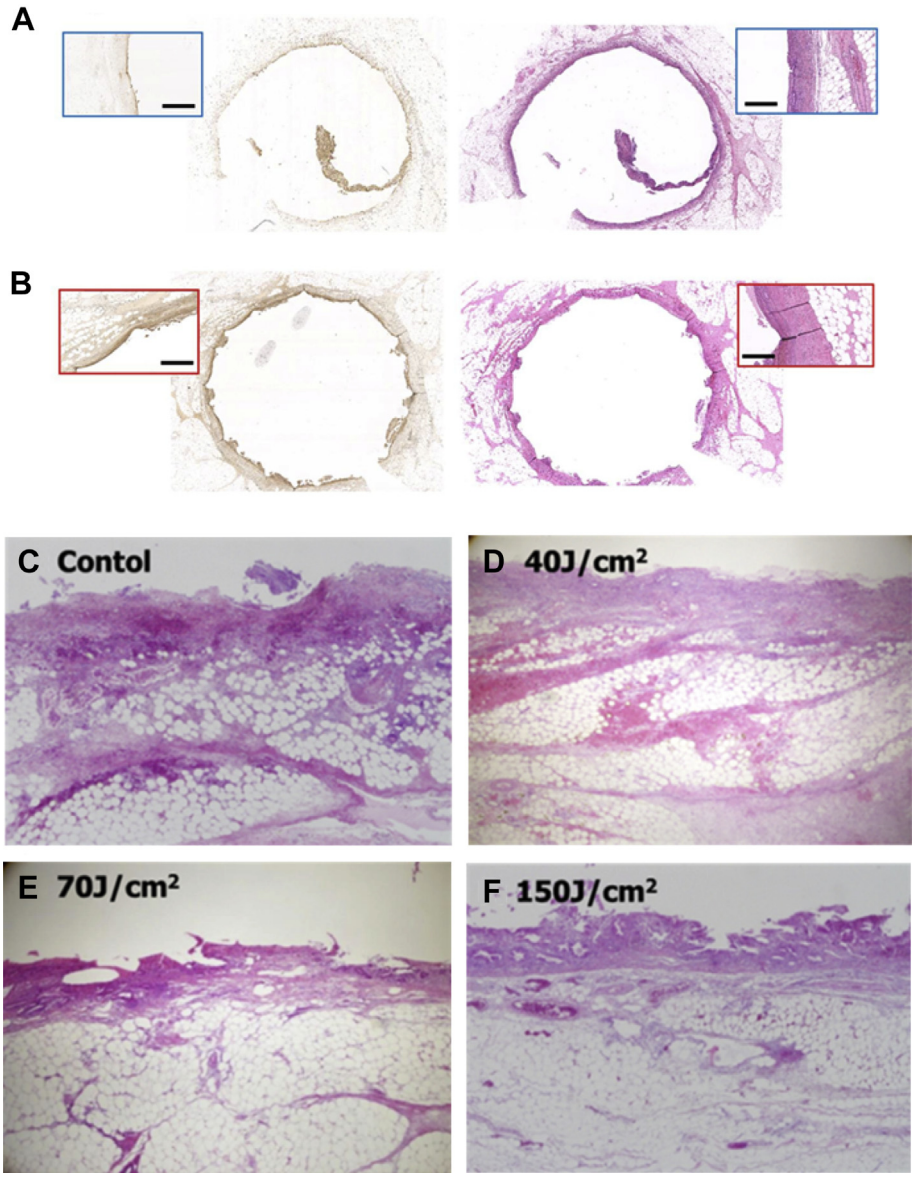

Fig. 6. Photodynamic activity and safety of PPA-stent after bile duct intervention on mini pigs. A) Light microscopy imaging of common bile duct from a swine model after conventional membrane-covered SEMS stenting, showing denuded mucosa with marked inflammation and hemorrhage due to mechanical injury from stent (H&E; 40×). B) Common bile duct pathological findings after the intervention of PDT-stent. C–F) Histological observation (200× magnification) of recovered bile duct with different endoscopic laser activation energy, C) non-activated control, D) 40 J/cm^2, E) 70 J/cm^2 and F) 150 J/cm^2.

relevant approach to treat cholangiocarcinoma as well as other gastrointestinal malignancies.

Acknowledgments

This research was supported by the Strategic Research through the National Research Foundation of Korea (NRF) grant funded by the Korea government (MSIP) (no. 2011–0028726) and Basic Science Research Program through the National Research Foundation of Korea (NRF) funded by the Ministry of Science, ICT and Future Planning (2014R1A2A2A04006562). Authors gratefully acknowledge support of National Center of Efficacy Evaluation for the Development of Health Products Targeting Digestive Disorders (NCEED).

Appendix A. Supplementary data

Supplementary data related to this article can be found at http://dx.doi.org/10.1016/j.biomaterials.2014.07.001.

References

[1] Khan SA, Davidson BR, Goldin RD, Heaton N, Karani J, Pereira SP, et al. Guidelines for the diagnosis and treatment of cholangiocarcinoma: an update. Gut 2012;61:1657–69.
[2] Patel T. Cholangiocarcinoma-controversies and challenges. Nat Rev Gastroenterol Hepatol 2011;8:189–200.
[3] Vauthey JN, Blumgart LH. Recent advances in the management of cholangiocarcinomas. Semin Liver Dis 1994;14:109–14.
[4] Sirica AE, Dumur CI, Campbell DJ, Almenara JA, Ogunwobi OO, Dewitt JL. Intrahepatic cholangiocarcinoma progression: prognostic factors and basic mechanisms. Clin Gastroenterol Hepatol 2009;7:S68–78.
[5] Patel T. Increasing incidence and mortality of primary intrahepatic cholangiocarcinoma in the United States. Hepatology 2001;33:1353–7.
[6] Matull WR, Khan SA, Pereira SP. Impact of classification of hilar cholangiocarcinomas (Klatskin tumors) on incidence of intra- and extrahepatic cholangiocarcinoma in the United States. J Natl Cancer Inst 2006;21(98):873–5.
[7] Parkin DM, Srivatanakul P, Khlat M, Chenvidhya D, Chotiwan P, Insiripong S, et al. Liver cancer in Thailand. I. A case-control study of cholangiocarcinoma. Int J Cancer 1991;48:323–8.
[8] Van Beers BE. Diagnosis of cholangiocarcinoma. HPB (Oxford) 2008;10:87–93.

[9] Valle J, Wasan H, Palmer DH, Cunningham D, Anthoney A, Maraveyas A, et al. Cisplatin plus gemcitabine versus gemcitabine for biliary tract cancer. N Engl J Med 2010;362:1273–81.
[10] Sasaki T, Isayama H, Nakai Y, Takahara N, Sasahira N, Kogure H, et al. Improvement of prognosis for unresectable biliary tract cancer. World J Gastroenterol 2013;19:72–7.
[11] Isayama H, Tsujino T, Nakai Y, Sasaki T, Nakagawa K, Yamashita H, et al. Clinical benefit of radiation therapy and metallic stenting for unresectable hilar cholangiocarcinoma. World J Gastroenterol 2012;18:2364–70.
[12] Anderson JE, Hemming AW, Chang DC, Talamini MA, Mekeel KL. Surgical management trends for cholangiocarcinoma in the USA 1998-2009. J Gastrointest Surg 2012;16:2225–32.
[13] Jarnagin WR, Shoup M. Surgical management of cholangiocarcinoma. Semin Liver Dis 2004;24:189–99.
[14] Farley DR, Weaver AL, Nagorney DM. "Natural history" of unresected cholangiocarcinoma: patient outcome after noncurative intervention. Mayo Clin Proc 1995;70:425–9.
[15] Kim JH. Endoscopic stent placement in the palliation of malignant biliary obstruction. Clin Endosc 2011;44:76–86.
[16] Raju RP, Jaganmohan SR, Ross WA, Davila ML, Javle M, Raju GS, et al. Optimum palliation of inoperable hilar cholangiocarcinoma: comparative assessment of the efficacy of plastic and self-expanding metal stents. Dig Dis Sci 2011;56:1557–64.
[17] Mukai T, Yasuda I, Nakashima M, Doi S, Iwashita T, Iwata K, et al. Metallic stents are more efficacious than plastic stents in unresectable malignant hilar biliary strictures: a randomized controlled trial. J Hepatobiliary Pancreat Sci 2012;20(2):214–22.
[18] Stoker J, Lameris JS, van Blankenstein M. Percutaneous metallic self-expandable endoprostheses in malignant hilar biliary obstruction. Gastrointest Endosc 1993;39:43–9.
[19] Lee MJ, Dawson SL, Mueller PR, Saini S, Hahn PF, Goldberg MA, et al. Percutaneous management of hilar biliary malignancies with metallic endoprostheses: results, technical problems, and causes of failure. Radiographics 1993;13:1249–63.
[20] Htay T, Liu MW. Drug-eluting stent: a review and update. Vascular health and risk management 2005;1:263–76.
[21] Zilberman M, Eberhart RC. Drug-eluting bioresorbable stents for various applications. Annu Rev Biomed Eng 2006;8:153–80.
[22] Tanaka T, Takahashi M, Nitta N, Furukawa A, Andoh A, Saito Y, et al. Newly developed biodegradable stents for benign gastrointestinal tract stenoses: a preliminary clinical trial. Digestion 2007;74:199–205.
[23] Kang SG. Gastrointestinal Stent Update. Gut Liver 2010;4:S19–24.
[24] Lee JW, Yang SG, Na K. Gemcitabine-releasing polymeric films for covered self-expandable metallic stent in treatment of gastrointestinal cancer. Int J Pharm 2012;427:276–83.
[25] Martinez JC, Puc MM, Quiros RM. Esophageal stenting in the setting of malignancy. ISRN Gastroenterol 2011;2011:719575.
[26] Manifold D, Maynard N, Cowling M, Machan L, Mason R, Adam A. Taxol coated stents in oesophageal adenocarcinoma. Gastroenterology 1998;114:A27.
[27] Moon S, Yang SG, Na K. An acetylated polysaccharide-PTFE membrane-covered stent for the delivery of gemcitabine for treatment of gastrointestinal cancer and related stenosis. Biomaterials 2011;32:3603–10.
[28] Witzigmann H, Berr F, Ringel U, Caca K, Uhlmann D, Schoppmeyer K, et al. Surgical and palliative management and outcome in 184 patients with hilar cholangiocarcinoma: palliative photodynamic therapy plus stenting is comparable to r1/r2 resection. Ann Surg 2006;244:230–9.
[29] Kahaleh M, Mishra R, Shami VM, Northup PG, Berg CL, Bashlor P, et al. Unresectable cholangiocarcinoma: comparison of survival in biliary stenting alone versus stenting with photodynamic therapy. Clin Gastroenterol Hepatol 2008;6:290–7.
[30] Berr F, Wiedmann M, Tannapfel A, Halm U, Kohlhaw KR, Schmidt F, et al. Photodynamic therapy for advanced bile duct cancer: evidence for improved palliation and extended survival. Hepatology 2000;31:291–8.
[31] Ortner ME, Caca K, Berr F, Liebetruth J, Mansmann U, Huster D, et al. Successful photodynamic therapy for nonresectable cholangiocarcinoma: a randomized prospective study. Gastroenterology 2003;125:1355–63.
[32] Na K, Shin D, Yun K, Park KH, Lee KC. Conjugation of heparin into carboxylated pullulan derivatives as an extracellular matrix for endothelial cell culture. Biotechnol Lett 2003;25:381–5.
[33] Lee JU, Jeong DY, Seo SG, Na K. Biodegradable nanogel based on all-trans retinoic acid/pullulan conjugate for anti-cancer drug delivery. J Pharm Inv 2013;43:63–9.
[34] Lee SJ, Park K, Oh YK, Kwon SH, Her S, Kim IS, et al. Tumor specificity and therapeutic efficacy of photosensitizer-encapsulated glycol chitosan-based nanoparticles in tumor-bearing mice. Biomaterials 2009;30:2929–39.
[35] Tomayko MM, Reynolds CP. Determination of subcutaneous tumor size in athymic (nude) mice. Cancer Chemother Pharmacol 1989;24:148–54.
[36] McAllister EW, Carey LC, Brady PG, Heller R, Kovacs SG. The role of polymeric surface smoothness of biliary stents in bacterial adherence, biofilm deposition, and stent occlusion. Gastrointest Endosc 1993;39:422–5.
[37] Weickert U, Venzke T, Konig J, Janssen J, Remberger K, Greiner L. Why do bilioduodenal plastic stents become occluded? A clinical and pathological investigation on 100 consecutive patients. Endoscopy 2001;33:786–90.
[38] Lee SS, Shin JH, Han JM, Cho CH, Kim MH, Lee SK, et al. Histologic influence of paclitaxel-eluting covered metallic stents in a canine biliary model. Gastrointest Endosc 2009;69:1140–7.
[39] Dumonceau JM, Heresbach D, Deviere J, Costamagna G, Beilenhoff U, Riphaus A. Biliary stents: models and methods for endoscopic stenting. Endoscopy 2011;43:617–26.
[40] O'Brien S, Hatfield AR, Craig PI, Williams SP. A three year follow up of self expanding metal stents in the endoscopic palliation of longterm survivors with malignant biliary obstruction. Gut 1995;36:618–21.
[41] Shingel KI. Current knowledge on biosynthesis, biological activity, and chemical modification of the exopolysaccharide, pullulan. Carbohydr Res 2004;339:447–60.
[42] Cheng KC, Demirci A, Catchmark JM. Pullulan: biosynthesis, production, and applications. Appl Microbiol Biotechnol 2011;92:29–44.
[43] Chan JY, Tang PM, Hon PM, Au SW, Tsui SK, Waye MM, et al. Pheophorbide a, a major antitumor component purified from Scutellaria barbata, induces apoptosis in human hepatocellular carcinoma cells. Planta Med 2006;72:28–33.
[44] Xodo LE, Rapozzi V, Zacchigna M, Drioli S, Zorzet S. The chlorophyll catabolite pheophorbide a as a photosensitizer for the photodynamic therapy. Curr Med Chem 2012;19:799–807.
[45] Hackbarth S, Horneffer V, Wiehe A, Hillenkamp F. Photophysical properties of pheophorbide-a-substituted. Chemical physics 2001;269:339–46.
[46] Castano AP, Mroz P, Hamblin MR. Photodynamic therapy and anti-tumour immunity. Nat Rev Cancer 2006;6:535–45.
[47] Gollnick SO, Brackett CM. Enhancement of anti-tumor immunity by photodynamic therapy. Immunol Res 2010;46:216–26.
[48] Mroz P, Szokalska A, Wu MX, Hamblin MR. Photodynamic therapy of tumors can lead to development of systemic antigen-specific immune response. PLoS One 2010;5(12):e15194.
[49] Castano AP, Mroz P, Hamblin MR. Photodynamic therapy and antitumor immunity. J Natl Cancer 2006;6(7):535–45.